

THE UNIQUE RAPID VARIABILITIES OF THE IRON $K\alpha$ LINE PROFILES IN NGC 4151

Jun-Xian Wang^{1,2}, Ting-Gui Wang^{1,2}, and You-Yuan Zhou^{1,2,3}

Received _____; accepted _____

¹Center for Astrophysics, University of Science and Technology of China, Hefei, Anhui, 230026, P. R. China; jxw@mail.ustc.edu.cn

²National Astronomical Observatories, Chinese Academy of Sciences

³Beijing Astrophysics Center, Beijing, 100080, P. R. China

ABSTRACT

We present a detailed analysis of the iron K α line variabilities in NGC 4151 by using long ASCA observation data obtained in May 1995. Despite the relatively small amplitude variations in the continuum flux, the iron K α line flux and profile show dramatic variations. Particularly, the line profile changes from single peak to seeming double peaks and back in time scales of a few 10^4 sec. The seemingly double-peaked profiles can be well interpreted as line emission from a Keplerian ring around a massive black hole. An absorption line at around 5.9 keV is also marginally detected. We discussed current Fe K line models, but none of them can well explain the observed line and continuum variations.

Subject headings: black hole physics — galaxies: active — galaxies: individual (NGC 4151) — line: profiles — X-rays: galaxies

1. Introduction

Broad Fe K fluorescence line profiles, detected in many AGNs (Tanaka et al. 1995, Nandra et al. 1997, Wang et al. 1999a, Nandra et al. 1999, and references therein), are thought to arise from the accretion disk near the center massive black hole of AGNs. The line profile, thus, carries important information about the distribution and kinematics of optically material as well as about the space properties in the vicinity of the postulated super massive black hole. Doppler and gravitational shifts would imprint characteristic signatures on the line profile which map the geometric and dynamical distributions of matter surround the black hole.

Additional information concerning the geometry of X-ray source and matter in the active nucleus could in principle be derived by studying the rapid variability (on time scales of several 10^4 s or less) of the line profile, intensity and their relationship with the continuum variations. So far, rapid variability in Iron K line has been detected in NGC 7314 (Yaqoob et al. 1996), MCG –6-30-15 (Iwasawa et al. 1996, 1999), NGC 4051 (Wang et al. 1999b) and NGC 3516 (Nandra et al. 1999).

The observed Fe $K\alpha$ line rapid variabilities in different targets or during different observations of the same target are quite different. Yaqoob el al. (1996) presented the evidence for rapid variability of the Fe K line profile in the narrow-line Seyfert galaxy NGC 7314, which is consistent with a disk-line of constant equivalent width superposed on a constant flux narrow line (presumably from the torus). Iwasawa et al. (1996) discovered that, during the ASCA observation on MCG –6-30-15 in 1994, when the source is bright, the Fe K line is weak and dominated by the narrow core, whilst during a deep minimum, a huge red tail appears. The intensity of broad Fe K line correlates inversely with the continuum flux on the time scales of several 10^4 s. And Iwasawa et al. (1999) discovered that during the ASCA observation on the same target in 1997, the Fe $K\alpha$ line of a flare

phase peaks around 5keV and most of its emission is shifted to below 6 keV with no component detected at 6.4keV. While for NGC 4051, during the ASCA observation in 1994, the equivalent width and the width of Fe K line correlate positively with the continuum flux (Wang et al. 1999b), which shows an opposite trend with the ASCA observation on MCG –6-30-15 in 1994. The rapid variabilities of Fe K α line profiles in NGC 3516 are also quite irregular (Nandra et al. 1999, Wang et al. 2000).

The nearby Seyfert 1.5 galaxy ($z = 0.0033$), NGC 4151, was first established as a bright X-ray source some thirty years ago (Gursky et al. 1971). Since that time, this archetypal low-luminosity active galaxy has invariably been considered as a prime target by all major X-ray astronomy missions. In 1995, NGC 4151 was observed by ASCA from May 10 to 12 (Leighly et al. 1997). The net exposure time of the observation is about 200 ks. Because of the enhanced sensitivity provided by ASCA and the much longer exposure time, the obtained Fe K α line profile has very high data quality (Wang et al. 1999a, here after W99). In this letter we report the discovery of unique and rapid variabilities of the iron line profiles in NGC 4151 during the ASCA observation in 1995.

2. Fitting the X-ray continuum

Only the SIS data are used in this paper to study the Fe K α line variabilities. Detailed description of the ASCA observation and data reduction can be found in W99. Figure 1a shows the background subtracted light curve (0.4 – 10.0 keV) with 256 s binning. Significant variability is absent on time scales of less than 1000s, but moderate variations can be seen on time scales of several 10^4 s, exhibiting a continuous slow drifting behavior (e.g. Lawrence 1980). The light curve shows an intensity dip at 60 ks from the beginning, which lasts about 50 ks, and two neighboring flares at about 150 ks, for which each lasts about 30 ks. The intensity ratios of the flares to the dip are around 0.8. Apart from these,

the count rate also increases slightly during the whole observation.

The time-averaged Fe K α line profile from this observation has been extracted by W99. The data quality of the line profile is one of the best that could be found in literatures (see Figure 1a in W99). In order to analysis the rapid variability properties of the Fe K α line profiles, we divide the whole observation into five time intervals (see Figure 1, I-1 to I-5). Following Weaver et al. (1994) and W99, we fit the underlying continuum of the each segment in the 1.0 – 4.0 and 8.0 – 10.0 keV bands (to exclude the broad iron line region) with a model which consists of a dual absorbed power law plus some fraction (the best-fit value for the time averaged spectrum is $\sim 5\%$) of the direct continuum scattered into our line of sight and absorbed only by the Galactic column of $2 \times 10^{20} \text{ cm}^{-2}$. We do not include a Compton reflection component in the spectral fits because of its small impact on the ASCA spectra. During the fitting, we fix the power law index and the flux of the scattered component at their best-fit values obtained from the time-averaged spectrum. Same to the time-averaged spectrum, the spectra of these five segments can also be well fitted by this model. We show the results in Table 1.

The power law indices for individual segments are all well consistent with the average value, i.e, there is no significant change in the continuum spectrum. However, the absorption columns density and the covering factor of the dual absorber showed significant variations (table 1), not correlated with variations of the continuum flux.

3. The Fe K α line profiles

Figure 2 shows the Fe K α line profiles for the whole observation and the five time intervals. The profiles are obtained from the ratio, the data divided by the best-fit continuum (folded through the detector response), multiplied by the power-law (original

form), thus are detector effective area corrected, and also independent from the model used to fitting the lines. The time-averaged line shows a strong narrow peak around 6.4 keV and a huge red wing extending to ~ 4.5 keV. Apart from a similar narrow core in the 6.4 keV, the line profile apparently differs by one interval to the other. The line profile of I-1 also shows a huge red wing, extending to about 4.0 keV with a possible red peak at around 4.9 keV; while for I-2, the red wing is much weaker. The line profile of I-5 is quite similar to the time averaged one. For I-3, besides the strong peak at 6.4 keV, there is also a seeming peak at around 5.4 keV. We noticed that between the two peaks there seems a valley in between which indicates that the line is double-peaked. The line profile of I-4 is similar to that of I-3, seemingly double-peaked, but much weaker. We conclude here that the Fe K α line profiles of NGC 4151 show clear and obvious variations during the ASCA observation.

Initially the line profiles are fitted with two gaussians and the results is given in Table 2. A narrow gaussian at around 6.4 keV and additional broad component can well fit the line profiles. and the results clearly present the variations of the line profiles and equivalent widths.

We also fit the Fe K line profiles with a model consist of a narrow component and a disk line (Fabian et al. 1989). The narrow core is likely emitted by material far away from the center black hole, such as torus, thus we would not expect substantial change in the line flux within the duration of the observation. During the fitting, we fix the flux of the narrow core for the five time intervals at the best-fit value from the time-averaged spectrum (which has a equivalent width of 70 eV according to the time-averaged spectrum). We also fix the disk-line energy at 6.4 keV in the source rest frame (W99), and fix the inclination angles of the disk at the best-fit value from the time-averaged spectrum. In fact, when we free the inclinations for the five time intervals, the best-fit values are all well consistent with that of the time-averaged spectrum (27 degree). As W99 did, the corresponding Fe K β and Ni K α

components (disk-line plus narrow core, see W99 for detail) are also included in the fit. The model can fit the line profiles quite well as the two Gaussians model do, and the results of the fit are shown in Table 3. We did not adopt the Model B in W99 because the scattered disk line component should be constant on such a short time scale, which is inconsistent with the rapid Fe K line variabilities we detected.

Nandra et al. (1999) claimed that they discovered a red shifted iron resonant absorption line at around 5.9 keV in the Fe K α profile of NGC 3516. We also add an additional absorption line component to the model, and find that including such a line can significantly improve the fit for I-4 ($\delta\chi^2 = 7$). However, the absorption line is not required for other segments ($\delta\chi^2 < 3.0$).

4. Discussion

4.1. The seemingly double-peaked line profiles

Massive black holes are generally thought to exist at the centers of active galaxies (Rees 1984), but unambiguous identification of a black hole has been impeded by lack of evidence for the strong-field relativistic effects expected in the vicinity of black holes. Because of its unique anticipated profiles, the Fe K α fluorescence line has long been considered as an observational key to the study of the innermost regions of active galactic nuclei (AGN). Fabian et al. (1989) and Laor (1991) pointed out that the line profiles from the accretion disk should be broad, skewed and double-peaked (dependent on the inclination of the disk and the line-producing region in the disk), which are characteristics of the Doppler effects of the accretion disk and the strong gravitational field in the vicinity of the central black hole.

The Fe K α line profiles detected in many AGNs have been proved to be skewed and extremely broad (Tanaka et al. 1995, Nandra et al. 1997, Wang et al. 1999a, Nandra et al.

1999, and references therein), consistent with the disk line model, so give the ever strongest evidence for the presence of massive black holes and accretion disks in the center of AGNs.

However, some alternative models, such as Comptonization and jet, can also explain the broad and skewed Fe K α line profiles. Those models do not require strong gravitational field and so give no support to the presence of massive black holes (Fabian et al. 1995, Misra & Sutaria 1999). But different to the disk line model, those models predict a smooth line feature, but not a double-peaked one. Though some indirect evidences have shown that they are not satisfactory (Fabian et al. 1995, Misra 2000, Reynolds & Wilms 2000), as Misra & Kembhavi (1998) have pointed out, we infer that the detection of a double-peaked line profile is the key to confirm the disk line model for the observed Fe K α lines, and so on confirm the detection of extremely strong gravitational field.

In this paper we find that the Fe K α line profile of NGC 4151 is seemingly double-peaked during phase I-3 and I-4 in Fig1. Because an additional resonant absorption line at 5.9 keV has also been detected in the line profile in I-4, we only focus on the profile of I-3 in this section. We show the seemingly double-peaked line profile of I-3 in detail in Fig.3, and the best-fit two gaussians and disk-line models are also plotted.

The seemingly double-peaked line profile strongly suggest that the line arises from materials with disk-like geometry. Additional strong gravitational field is also needed to explain the red shift of the profile. Others models for the broad line profiles, such as Comptonization or jet, can not be responsible for a double-peaked line profile, and disk-like outflows or inflows with high velocity can not be responsible for the red shift of the line profile. The best disk line fits show that the line mainly arises from a narrow ring between $10.8 R_g$ and $18.6 R_g$.

Currently, perhaps due to the limited energy resolution and data quality, obvious double-peaked Fe K α line profile has never been detected in any active galactic nuclei.

We noticed that the line profile of MCG –6-30-15 in Fig. 1b of Wang et al. (1999a) looks double-peaked, but the plot was folded through the effective area of the detectors which rises sharply towards the low energy, so did not give the true profile of the line. While in plotings corrected for detectors' effective area, we can not see obvious double peaks (see Fig. 7 of Iwasawa et al. 1996 and Fig. 6 of Fabian et al. 2000). We hope that the new generation X-ray satellites, such as XMM, can show us clearly double-peaked iron line profiles of AGNs.

4.2. The rapid variabilities of the Fe K α line profiles

Additional to the double-peaked line profiles, the rapid variabilities of the Fe K line profiles in NGC 4151 are also detected in this letter. We divided the whole ASCA observation of NGC 4151 in 1995 into five time intervals, and found that, despite the relatively small amplitude variations in the continuum flux, the Fe K α line flux and profiles show dramatic variations: during the first time interval I-1, the iron line profile is broad and skewed, showing a strong peak at 6.4 keV, and a huge red wing extending to ~ 4.5 keV, similar to the time-averaged line profile; after several 10^4 s, the huge red wing becomes very weak (I-2); for I-3, except the strong peak at 6.4 keV, there is also a seeming peak at around 5.4 keV; the line profile of I-4 is similar to that of I-3, but much weaker; and finally, the line profile change back to single peak (I-5). The line equivalent widths of the five intervals are 375, 148, 329, 168 and 300 eV respectively, showing obvious variations.

The rapid variabilities of Fe K line profiles discovered previously have suggested that the X-ray continuum flux is generated by magnetic flares above the accretion disk, and at any given time there are only a few flares moving around above the disk (Iwasawa et al. 1996, Fabian 1997, Wang et al. 1999b, Iwasawa et al. 1999, Wang et al. 2000). Flares with different location and different motion can give different fluorescence line profiles.

Can the magnetic flare model also explain the observed rapid variabilities of Fe K α line in NGC 4151? For I-1 and I-5, the X-ray continuum (in the flare model context) could be dominated by a single or several strong flares located very close to the center black hole, while the inner disk radius from the disk line fits (7.4 and 8.3 R_g) gives strong supports to this model. For I-2, the X-ray continuum seems to be dominated by flares far away from the center black hole ($R_i = 17 R_g$). For I-3 and I-4, the X-ray continuum could be dominated by a single or several strong flares, which are $\sim r_g$ above and coroating with the disk at around $14 R_g$, with only the materials in the ring around $14 R_g$ being illuminated. The large dramatic decreasing in the line EWs from I-3 to I-4 might be due to different degree of the anisotropy in the X-ray continuum, i.e., larger fraction of the X-ray continuum received by the disk in I-3 than in I-4. However, it requires some fine tune in order to keep the observed continuum more or less constant. Alternatively, Misra (2000) suggested that the changes in the disk structure may explain the observed line profile variations, but, a disk undergoing structure changes is also hard to keep the same radiative spectrum. Finally, the decreasing of the fluorescent yielding may be due to the increasing ionization in the disk skin. Under flare context, large change in the ionization structure of disk skin is possible even for quite moderate variations in the observed continuum flux if the flares have different heights. If this is case, we would expect that the flare is lower in the I-4 than in I-3. This should also reflect in the line profile. However, the uncertainty in the disk parameters do not allow us to verify this.

The observed properties strongly suggest that the rapid line variations may not be due the variations of X-ray continuum source. Instead, it may be due to changes in geometry or ionization level of the reflecting medium and at the same time, these changes should not affect the X-ray producing medium. If so, except for the variations of the X-ray continuum source, what can lead to the changes in geometry or ionization level of the reflecting medium?

An absorption line at 5.8 keV is marginally detected in I-4, but not significant in other intervals. Note a variable absorption line at the same energy has been discovered by Nandra et al. (1999) in NGC 3516. Nandra et al. (1999) interpreted this line as the redshifted Fe K resonant absorption line. The large redshift is either caused by the infalling absorbing material or by the strong gravity in the vicinity of the black hole. Given the fact that the line is highly variable and the large redshift, the agreement of the redshifts in this two objects perhaps is not purely coincidence, but have some physical origin. If so, the gravitational redshift explanation would be favored.

This work is supported by Chinese National Natural Science Foundation, Chinese Science and Technology ministry and Foundation of Ministry of Education.

REFERENCES

Fabian, A. C., Rees, M. J., Stella, L. & White, N. E. 1989, MNRAS, 238, 729

Fabian, A. C., et al. 1995, MNRAS, 277, L11

Fabian, A. C. 1997, X-ray Imaging and spectroscopy of cosmic hot Plasmas, Univ. Acad. Press, 201

Fabian, A. C. Iwasawa, K., Reynolds, C. S. & Young, A. J. 2000, PASP review, astro-ph0004366

Gursky, H., Kellogg, E. M., Leong, C., Tananbaum, H. & Giacconi, R. 1971, ApJ, 165, L43

Iwasawa, K., et al. 1996, MNRAS, 282, 1038

Iwasawa, K., Fabian, A. C., Young, A. J., Inoue, H. & Matsumoto C. 1999, MNRAS, 306, L19

Laor, A. 1991, ApJ, 376, 90

Lawrence, A. 1980, MNRAS, 192, 83

Leighly, K. M., et al. 1997, X-ray Imaging and spectroscopy of cosmic hot Plasmas, Univ. Acad. Press, 291

Misra, R. & Kembhavi, A. K. 1998, ApJ, 499, 205

Misra, R. & Sutaria, F. K. 1999, ApJ, 517, 661

Misra, R. 2000, submitted to MNRAS, astro-ph9912178

Nandra, K., George, I. M., Mushotzky, R. F., Turner, T.J. & Yaqoob, T. 1997, ApJ, 477, 602

Nandra, K., George, I. M., Mushotzky, R. F., Turner, T.J. & Yaqoob, T. 1999, ApJ, 523, L17

Rees, M. J. 1984, ARAA, 22, 471

Reynolds, C. S. & Wilms, J. 2000, 533, 821

Tanaka, Y., et al. 1995, *Nature*, 375, 659

Wang, J. X., Zhou & Wang, T. G. 1999a, *ApJ*, 523, L129 (W99)

Wang, J. X., Zhou, Y. Y., Xu, H. G. & Wang, T. G. 1999b, *ApJ*, 516, L65

Wang, T. G. et al. 2000, in preparation

Yaqoob T., Serlemitsos P.J., Turner T.J., George I.M. & Nandra K. 1996, *ApJ*, 470, L27

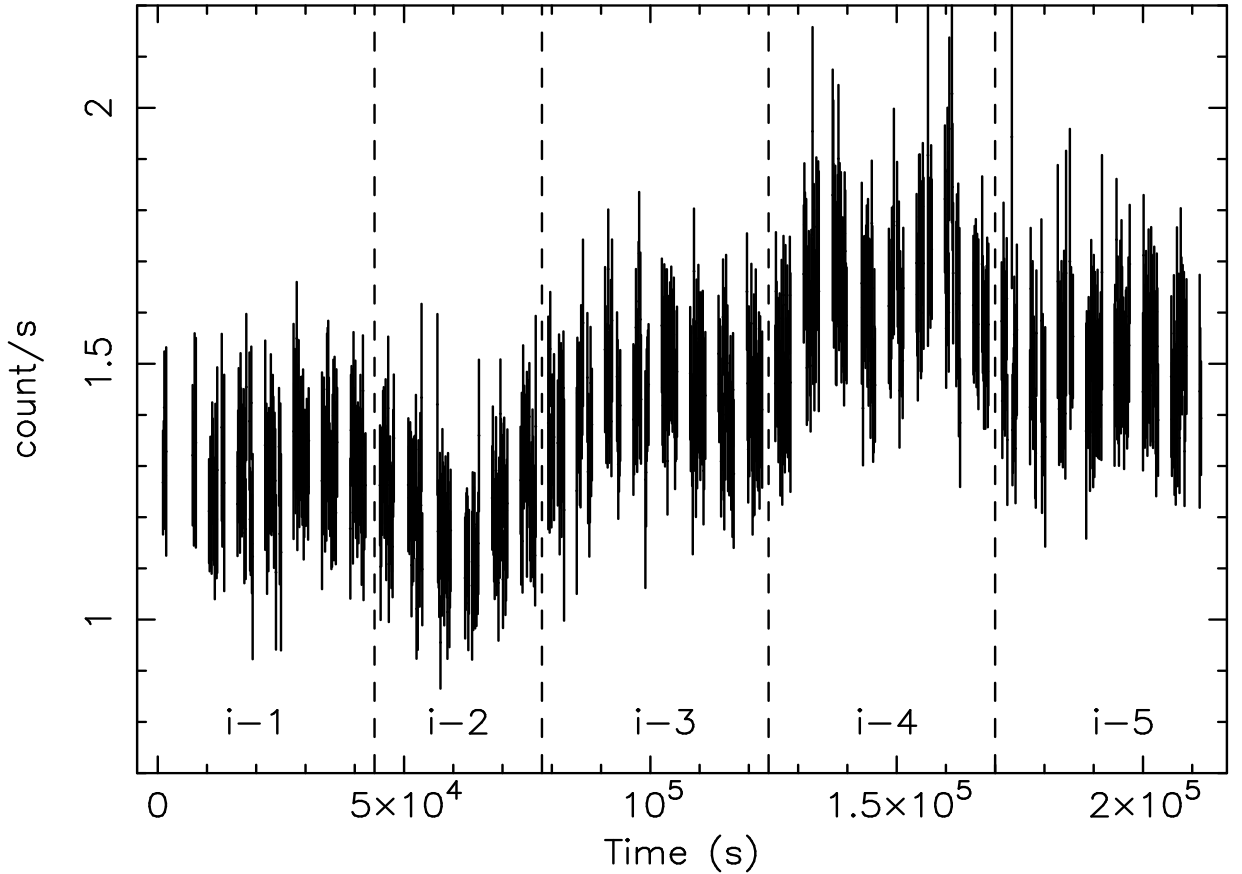


Fig. 1.— Background-subtracted light curve (0.4 – 10.0 keV, SIS) of NGC 4151 for the long ASCA observation taken in May 1995. The light curve is binned using 256 s time intervals. The background were estimated from source-free regions. The five time intervals are also shown here.

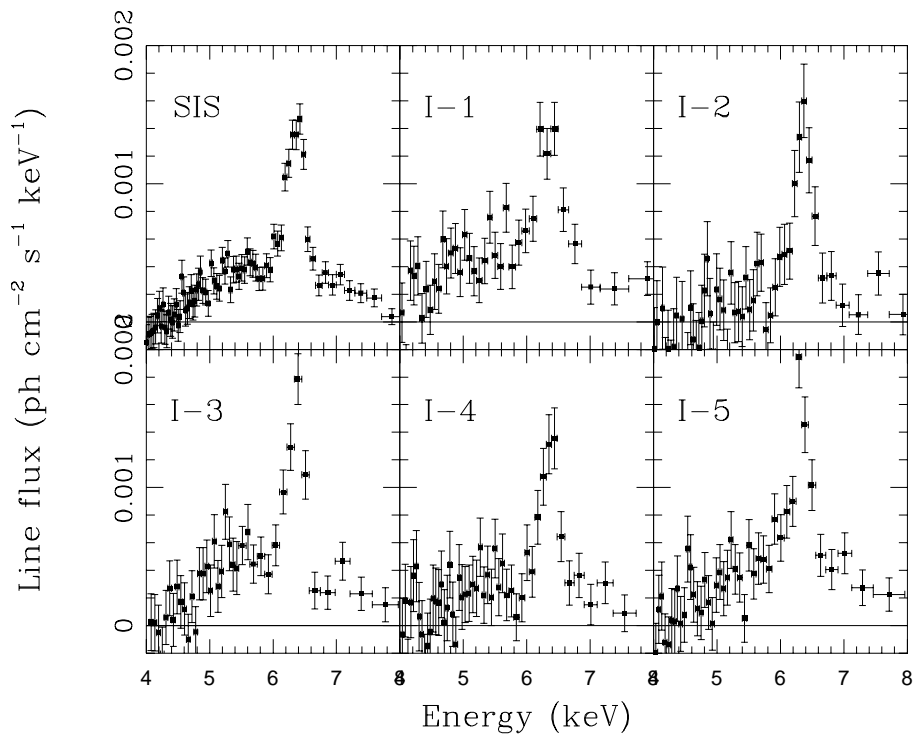


Fig. 2.— The Fe K α line profiles for the five time intervals. see text for details.

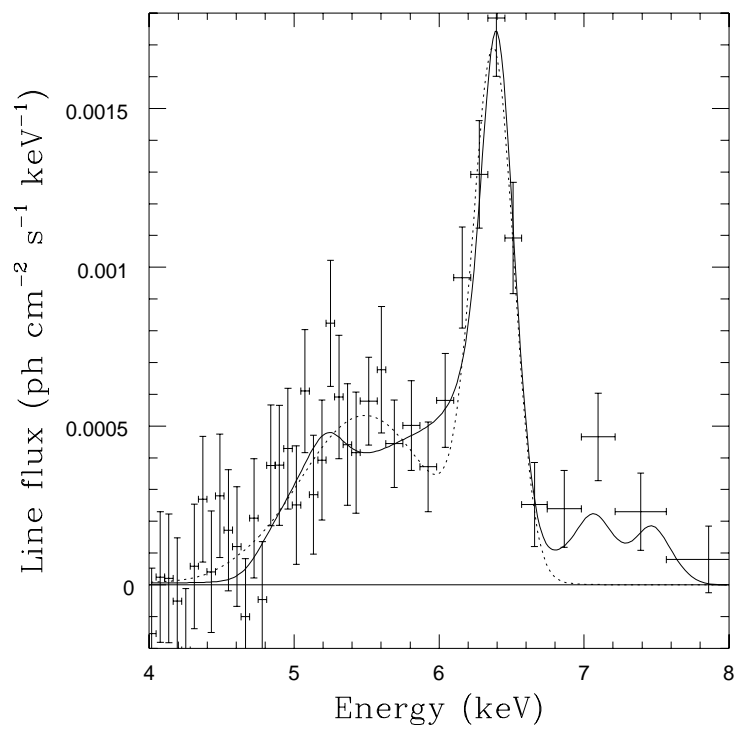


Fig. 3.— The line profile of I-3. dotted line: best-fit two gaussians; solid line: best-fit disk-line model.

Table 1: Dual absorbed power law fits for the 1.0 – 10.0 keV continuum of the five time intervals

intervals(ks)	NH1	NH2	cover factor	index	flux ^a	χ^2/dof
0. - end	$3.17^{+0.15}_{-0.15}$	$7.44^{+1.03}_{-0.99}$	$0.62^{+0.04}_{-0.05}$	$1.34^{+0.06}_{-0.07}$	2.292	638/570
0. - 42	$3.29^{+0.50}_{-0.60}$	$7.92^{+3.95}_{-2.97}$	$0.60^{+0.10}_{-0.11}$	$1.23^{+0.22}_{-0.19}$	2.123	457/441
42. - 75.	$3.26^{+0.49}_{-0.51}$	$10.17^{+3.32}_{-2.73}$	$0.73^{+0.05}_{-0.07}$	$1.50^{+0.25}_{-0.22}$	2.322	485/434
75. - 122.	$3.06^{+0.45}_{-0.51}$	$6.73^{+2.14}_{-1.61}$	$0.69^{+0.08}_{-0.08}$	$1.36^{+0.15}_{-0.14}$	2.424	477/452
122. - 168.	$3.43^{+0.33}_{-0.37}$	$10.06^{+4.46}_{-4.39}$	$0.49^{+0.11}_{-0.12}$	$1.34^{+0.24}_{-0.19}$	2.810	415/456
168. - end	$2.43^{+0.37}_{-0.39}$	$6.06^{+1.48}_{-1.19}$	$0.73^{+0.06}_{-0.06}$	$1.31^{+0.13}_{-0.13}$	2.409	411/449

^a 10^{-10} erg/cm².s (flux of 2.0 – 10.0 keV, absorption corrected)

Table 2: Two Gaussians fits for the Fe K α line of the five time intervals. The parameters are central energy (E_c), width (σ) and equivalent width (EW) for two Gaussians. The equivalent widths are calculated relative to the X-ray continuum at 6.4 keV

intervals	E_c1 (keV)	$\sigma1$ (keV)	EW1 (eV)	E_c2 (keV)	$\sigma2$ (keV)	EW2 (eV)	χ^2/dof
SIS	$6.38^{+0.01}_{-0.01}$	$0.08^{+0.02}_{-0.03}$	140^{+16}_{-17}	$6.03^{+0.10}_{-0.09}$	$0.87^{+0.09}_{-0.08}$	374^{+36}_{-34}	1198/1118
I-1	$6.39^{+0.05}_{-0.05}$	$0.15^{+0.06}_{-0.06}$	164^{+69}_{-52}	$5.89^{+0.22}_{-0.31}$	$0.95^{+0.21}_{-0.20}$	484^{+100}_{-91}	965/889
I-2	$6.39^{+0.03}_{-0.03}$	$0.00^{+0.09}_{-0.00}$	117^{+25}_{-51}	$6.36^{+0.26}_{-0.23}$	$0.36^{+0.39}_{-0.15}$	149^{+60}_{-69}	914/858
I-3	$6.40^{+0.02}_{-0.02}$	$0.10^{+0.03}_{-0.04}$	215^{+37}_{-56}	$5.51^{+0.10}_{-0.10}$	$0.44^{+0.11}_{-0.09}$	220^{+40}_{-41}	927/917
I-4	$6.37^{+0.03}_{-0.03}$	$0.12^{+0.04}_{-0.12}$	166^{+27}_{-27}	$5.40^{+0.13}_{-0.17}$	$0.33^{+0.23}_{-0.15}$	83^{+53}_{-30}	840/925
I-5	$6.35^{+0.02}_{-0.03}$	$0.00^{+0.07}_{-0.00}$	121^{+32}_{-25}	$6.23^{+0.18}_{-0.18}$	$0.87^{+0.20}_{-0.16}$	401^{+72}_{-71}	856/910

Table 3: Disk line fits for the Fe K α line of the five time intervals

intervals	R _i (R _g)	R _o (R _g)	EW(eV)	q	χ^2/dof
SIS	8.8 ^{+0.8} _{-0.9}	1000 ^f	304 ⁺¹⁷ ₋₁₇	-4.4 ^{+0.9} _{-0.7}	1201/1119
I-1	7.4 ^{+0.8} _{-0.6}	1000 ^f	375 ⁺⁴² ₋₄₁	-4.2 ^{+0.6} _{-0.8}	975/892
I-2	16.8 ^{+45.4} _{-10.7}	1000 ^f	148 ⁺⁴⁴ ₋₄₀	-2.3 ^{+0.6} _{-0.9}	918/861
I-3	10.8 ^{+1.7} _{-4.8}	18.6 ^{+3.8} _{-2.9}	330 ⁺³⁷ ₋₃₇	-2 ^f	917/920
I-4	9.1 ^{+3.4} _{-3.1}	18.5 ^{+9.2} _{-5.2}	171 ⁺³¹ ₋₃₁	-2 ^f	839/928
I-5	8.3 ^{+1.1} _{-1.1}	1000 ^f	300 ⁺³³ ₋₃₃	-4.3 ^{+1.0} _{-2.6}	871/913

^f frozen because the fit can not give sufficient constraints on the parameters.